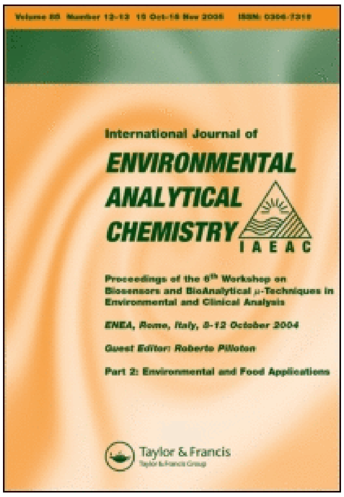

International Journal of Environmental Analytical Chemistry
Publication details, including instructions for authors and subscription information:
http://www.informaworld.com/smpp/title~content=t713640455

Ground-based on-line measurements of peroxyacetyl nitrate (PAN) and peroxypropionyl nitrate (PPN) in the Pearl River Delta, China

Bin Wang[a]; Min Shao[a]; James M. Roberts[b]; Guang Yang[a]; Fan Yang[a]; Min Hu[a]; Limin Zeng[a]; Yuanhang Zhang[a]; Jianbo Zhang[a]
[a] State Joint Key Laboratory of Environmental Simulation and Pollution Control, College of Environmental Science and Engineering, Peking University, Beijing 100871, China [b] NOAA/ESRL Chemical Sciences Division, and Cooperative Institute for Research in the Environmental Sciences, University of Colorado, Boulder 80305, CO, USA

To cite this Article Wang, Bin , Shao, Min , Roberts, James M. , Yang, Guang , Yang, Fan , Hu, Min , Zeng, Limin , Zhang, Yuanhang and Zhang, Jianbo(2010) 'Ground-based on-line measurements of peroxyacetyl nitrate (PAN) and peroxypropionyl nitrate (PPN) in the Pearl River Delta, China', International Journal of Environmental Analytical Chemistry, 90: 7, 548 — 559

To link to this Article: DOI: 10.1080/03067310903194972

URL: http://dx.doi.org/10.1080/03067310903194972

Intern. J. Environ. Anal. Chem.
Vol. 90, No. 7, 15 June 2010, 548–559

Taylor & Francis
Taylor & Francis Group

Ground-based on-line measurements of peroxyacetyl nitrate (PAN) and peroxypropionyl nitrate (PPN) in the Pearl River Delta, China

Bin Wang[a], Min Shao[a], James M. Roberts[b], Guang Yang[a], Fan Yang[a], Min Hu[a], Limin Zeng[a], Yuanhang Zhang[a] and Jianbo Zhang[a]*

[a]*State Joint Key Laboratory of Environmental Simulation and Pollution Control, College of Environmental Science and Engineering, Peking University, Beijing 100871, China;* [b]*NOAA/ESRL Chemical Sciences Division, and Cooperative Institute for Research in the Environmental Sciences, University of Colorado, Boulder 80305, CO, USA*

(*Received 26 November 2008; final version received 25 June 2009*)

Aiming at understanding the regional O_3 problem and the impacts of city to rural areas, ambient peroxyacetyl nitrate (PAN) and peroxypropionyl nitrate (PPN) were measured by an on-line instrument at a back garden site (BGS), and a receptor site for urban plume from Guangzhou city. The highest mixing ratios for PAN and PPN were 3.9 and 0.7 ppbv, respectively. PAN and PPN had a similar diurnal pattern as that of O_3. As revealed by the slope of the linear regression line between PPN and PAN, anthropogenic volatile organic compounds (AVOCs) dominated photochemical O_3 production most of the time. From the correlation between PAN and O_3, the regional background level of O_3 was derived to be 28 ± 15 ppbv. Two night-time plumes containing elevated PAN and O_3 were observed, and the backward-trajectory analysis supported the transport of urban plume from Guangzhou city. Based on the temporal variation of PPN/PAN, two day-time episodes were also selected to discuss the influence from Guangzhou.

Keywords: PAN; PPN; regional ozone pollution; transportation; PRD

1. Introduction

The Pearl River Delta (PRD) is one of the most economically developed areas in China. It is located in the southern part of the mainland as shown in Figure 1. In the past two decades, with the rapid growth in economy and vehicle population, the PRD region has been suffering from serious air quality problems, especially O_3 pollution [1]. In Hong Kong, the highest hourly average of 171 ppbv had been recorded [2]. At Tai O, a costal site which is 32 km west of the centre of Hong Kong, the highest hourly averages of 142 ppbv and 189 ppbv were observed in November 2001 and July 2002, respectively [1,3]. However, the formation mechanism of ground level O_3 was not adequately investigated in this area. As a co-product of O_3, peroxyacyl nitrates ($RC(O)OONO_2$, PANs) could be indicators for understanding O_3 formation processes.

In fact, PANs were first identified in Los Angeles photochemical smog, and received a lot of attention as a tracer for secondary air pollutants, and also for their negative effects on human health, crop yield, and forest productivity [4–7]. PAN ($CH_3C(O)OONO_2$) and PPN ($CH_3CH_2C(O)OONO_2$) are the most abundant species in the PANs family [8,9].

---

*Corresponding author. Email: jbzhang@pku.edu.cn

ISSN 0306–7319 print/ISSN 1029–0397 online

DOI: 10.1080/03067310903194972
http://www.informaworld.com

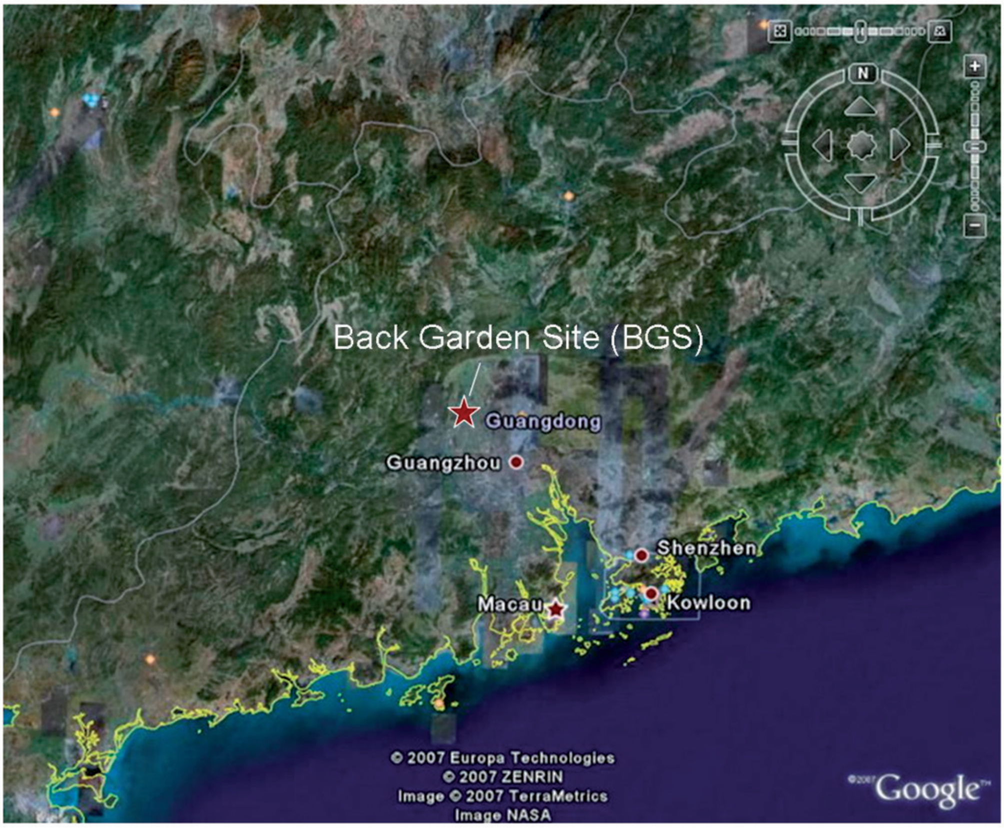

Figure 1. Location of the Back Garden Site in the Pearl River Delta (map from Google Earth).

Quantification of PANs was complex work, since they were a kind of short-life trace gases prone to thermo-destruction. Results from off-line measurement in China were reported only once so far [10]. On-line methods were reported in late 1990s. They quantified PAN in every 5–10 minutes, and the detection limits were about 5–50 pptv [e.g. 11,12]. On-line measurements of PAN in China were also reported recently [12,13]. This manuscript presents the first online PAN and PPN measurements in PRD. We employed a state-of-the-art online GC-ECD system (gas chromatography equipped with an electron capture detector) from NOAA (Boulder, CO.). Air samples were injected every 5 minutes, and the detection limits were 5 pptv for PAN and PPN. It is the fastest online PANs analytical GC system with the lowest detection limits so far.

As co-products of photochemistry, O_3, PAN, and PPN are closely linked to each other, and high correlations are usually found among these species. From the intercept of the ratio of O_3 *versus* PAN, the background level of O_3 can be estimated [14,15]. Based on the slope of the linear regression line of PPN/PAN, the predominant sources (anthropogenic or biogenic) of precursor VOCs of O_3 can be identified [15–17]. Even though the life time of PAN is generally short under ambient conditions, in some cases, they can be well preserved and transported to downwind regions [18–21]. As an intermediate reservoir for nitrogen oxides (NOx) and organic peroxy radicals (RO_2), PAN can release these pollutants and cause serious pollution remote areas [18,22–25].

To understand the regional O_3 chemistry in the Pearl River Delta region, a field campaign, PRIDE-PRD 2006, was organised in summer 2006. The ambient concentrations of PAN, and PPN, together with NOx, CO, O_3, non-methane hydrocarbons (NMHCs), and free radicals (ROx), were continuously measured. The role of anthropogenic and natural VOCs in ozone formation was explored by the relationship between PAN and PPN, and the influence of local chemistry *versus* transport.

2. Experimental

2.1 *Site description*

BGS (113.02°E, 23.28°N) is located at a rural area in the Pearl River Delta (PRD) in the south of China, which is about 60 km to the northwest of Guangzhou city, as shown in Figure 1. The sampling site was set up on top of a 3-floor building surrounded by trees, farmlands, and a reservoir. There were no industries in vicinity of the site. As the prevailing wind is from the south or southeast in summer, BGS was selected as a receptor site to study the impacts of urban plume from Guangzhou.

2.2 *Instrumentation*

An on-line gas chromatography equipped with an electron capture detector (GC-ECD) was used to do the PAN, PPN measurements in the PRIDE-PRD campaign. It was on loan from the Chemical Sciences Division of the Earth System Research Laboratory (ESRL) of National Oceanic and Atmospheric Administration (NOAA), and was employed in a series of field studies in USA [16,17,24,26].

Ambient air samples were drawn through the main inlet, which was a 6-metre long PFA tubing (0.5 inch, ID) with one end connecting to a pump and the other end setting at about 3 metres above the top of a 3-floor building. A small flow was drawn into the GC injection valve, through a 0.125 inch ID PFA tube. Both the main flow and the branch flow were controlled by mass flow controllers (MFC), with the flow rates setting at 1 standard litre per minute (slpm) and 20 standard cubic centimetres per minute (sccm), respectively. Two ambient cc was injected for each sample. The temperatures of the capillary column (RTX-200, Restek) and the ECD detector (Shimadzu, mini-2) were consistently controlled at 15°C and 40°C under operating conditions (more specific information can be found in [11]).

Gaseous PAN standard was synthesised in a 'Photo-source' cell. PAN was made photochemically via the 285 nm photolysis of acetone in the presence of a calibrated NO flow. The flow rates of NO and acetone were set to 1 sccm and 40 sccm by MFCs, respectively. The concentration of NO and acetone were both 1.01 ppmv (Scott Specialty Gases). Since acetone was always in excess in this system, the PAN concentration was determined by the NO standard concentration and flow rate, and the conversion efficiency of $93 \pm 5\%$. Dilution air was made by ambient air. During calibrations, the ambient air was diverted through a decomposition chamber heated to 125°C prior to entering the sample loop. The chamber consisted of a 2.1-m length of 4-mm ID Teflon PFA tubing, sufficient to provide at least 99% decomposition of PAN and PPN their parent peroxyacyl radical and NO_2.

PPN was synthesised in the liquid phase following the method described by [11]. The resulting mixture was placed in a diffusion cell, which was used to produce a stable concentration of PPN in the sample stream. The outflow first went to NOy instrumentation to quantify the concentrations of PPN, and then switched to PANs instrument for calibration [11]. The detection limits for both PAN and PPN were 5 pptv, and the method uncertainties in the measurements is ±15% for PAN and ±20% for PPN. Generally the calibrations were carried out during midnight, because the ambient PAN and PPN mostly peaked in the afternoons [14,27,28].

Ambient PAN and PPN levels were continuously measured from 0:00 on 7 July to 24:00 on 30 July, with a time resolution of 5 minutes during the whole campaign, and 5826 valid data points were obtained.

2.3 *Quality assurance and quality control*

Before measurements, the instrument was checked by zero gas which was the dilution air described above. The responses of PAN and PPN were actually zero, indicating no interferent was contained in the instrument. Since PAN and PPN were sensitive to thermodestruction, the room temperature of the lab was strictly controlled at $20 \pm 4°C$, contributing a variation of less than 1.5% to the volume of injected air samples, according to Clapyron equation. On-line system calibrations were performed roughly every 3 days, and the response factor of PAN and PPN were varied in a range of 9%. The detection limits were identified by [11], and the data below this limit were excluded for interpretation and discussion.

3. Results and discussion

3.1 *Mixing ratios of PAN and PPN*

Figure 2 shows the diurnal variations of PAN and PPN. During the campaign, the highest mixing ratios for PAN and PPN were 3.9 ppbv and 0.7 ppbv, the mean levels were 1.32 ppbv and 0.21 ppbv (Figure 2a and b), and the lowest values were both under detection limits of 5 pptv. These results are comparable to those observed in Beijing in the summer of 2005 [13], but much lower than the concentrations measured in Mexico City and Santiago [14,28].

PAN and PPN showed strong diurnal patterns. The daily maximum mixing ratios were usually detected in the afternoon, and the minimum levels generally occurred at about 6:00 am (Local Time, LT). However, two night-time peaks of PAN and PPN were observed during the campaign, and O_3 also increased at the same time (Figure 2c and d).

3.2 *The correlation between PAN and PPN*

PAN and PPN are co-products of VOCs-NOx photochemistry, and strongly correlated with each other. The result of this study is shown in Figure 3, the linear regression coefficient R was 0.96. PAN can be formed by VOCs from both anthropogenic and biogenic origins, while the VOC precursors for PPN are solely from anthropogenic origin [16,29–31]. Therefore, the slope of the linear regression line between PPN and PAN will provide an approach to evaluate the relative importance of manmade and natural VOCs in photochemistry. The use of this relation as a general indicator has been intensively discussed by Roberts *et al.* [17,26], the ratio PPN/PAN between 13.5% and 17.2% indicates AVOCs dominance, while the ratio lower than 10% stands for

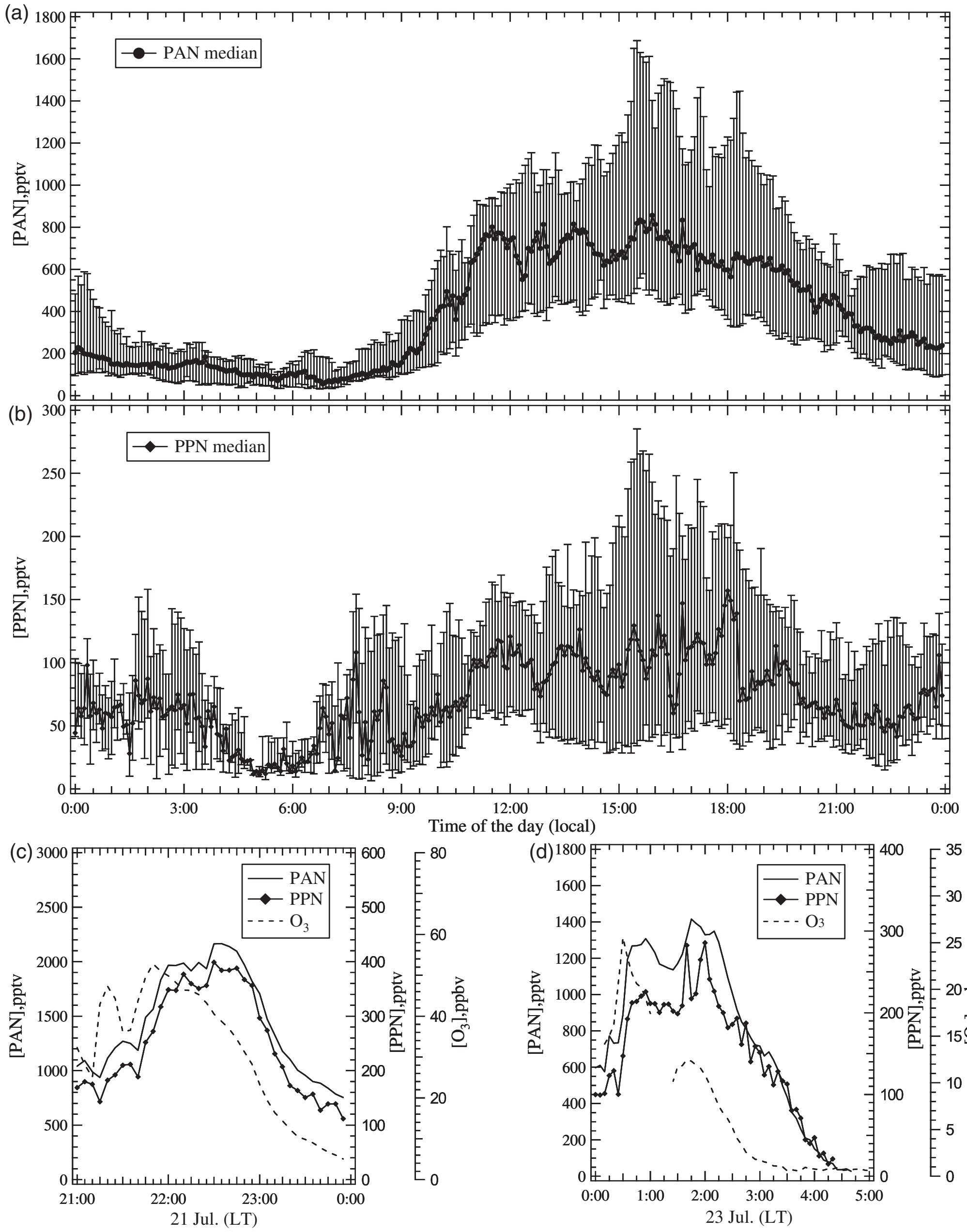

Figure 2. Diurnal variations of (a) PAN and (b) PPN. Black solid circles and squares are the medians of PAN and PPN, respectively. The error bars in each panel are the percentiles of 25% (lower limits) and 75% (upper limits). Figure 2(c) and (d) show night-time peaks of PAN and PPN on 21 July and 23 July, respectively. In each panel PAN is shown by a solid line and PPN is shown by a dashed line.

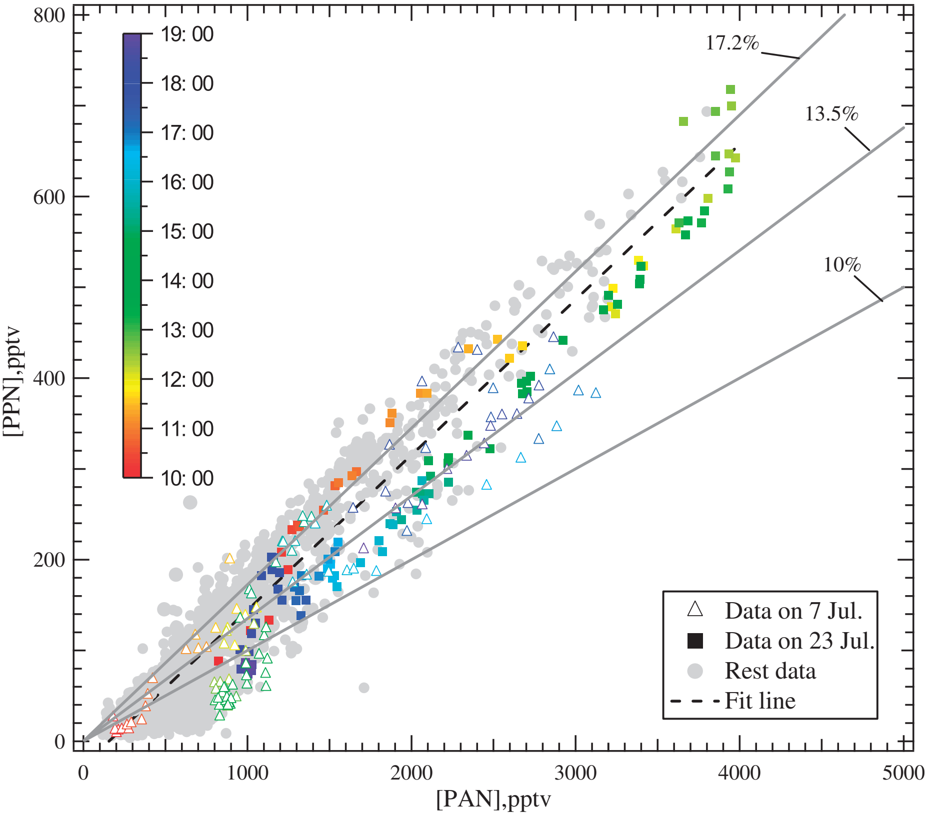

Figure 3. Correlation between PPN and PAN. The solid grey circles show the data from 10:00 to 19:00 of the whole campaign except 7 July and 23 July which are demonstrated by open triangles and solid squares, respectively. The data on these two days are also interpreted by time colour-scales. The dashed line is the fit line of the correlation between PPN and PAN; the two solid lines are trend lines of 17.2%, 13.5% and 10%.

BVOCs dominance. The overall ratio of this study was 17%, lying very close to the upper trend line of 17.2% (Figure 3), suggesting that AVOCs were dominating the photochemical production of O_3 at BGS.

3.3 *O_3 and PAN*

Figure 4 shows the temporal profiles of O_3 and PAN. They usually peaked in the afternoon and then decreased till next sunrise. On 7 of the 23 sampled days, the mixing ratios of O_3 exceeded the second level criterion of the Chinese National Ambient Air Quality Standards (NAAQS, 80 ppbv). On 4 of the 7 days, 10, 18, 23 and 24 July, high levels of PAN were also measured. The ratios between the daily maximum of PAN and O_3 were 1/36, 1/28, 1/43, and 1/33, respectively. The highest mixing ratios of PAN and O_3 in this campaign were both measured on 23 July, which were 3.9 ppbv and 141 ppbv (hourly average). On the other 3 days, 12, 20 and 21 July, the levels of PAN were much lower. The ratios of PAN/O_3 were 1/65, 1/66, and 1/68, respectively.

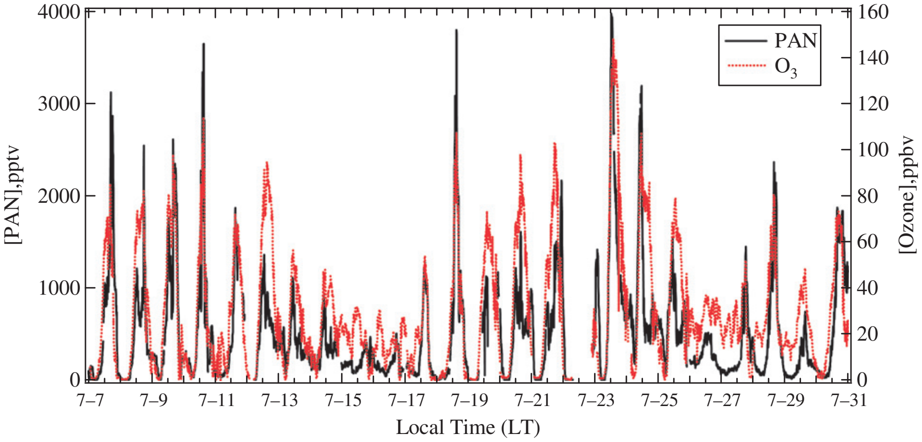

Figure 4. Temporal profiles of PAN and Ozone. The grey dashed line is PAN and the red dotted line is Ozone.

Since O_3 could be formed nearly by all reactive VOCs but PAN could only be produced by precursors to PA radicals ($CH_3C(O)OO$), the correlation between their daily maximums could reveal the composition of the precursor VOCs and provide useful information on the formation processes of PAN and O_3. The values on the violation days of this study fell into two groups, the averages of which were 0.029 and 0.015, respectively, indicating that, on average, 14 more PAN molecules were produced for per 1000 O_3 molecules formed in the airshed on 10, 18, 23 and 24 July than those on 12, 20 and 21 July. Similar ratios were reported for other areas, e.g. Mexico City (0.02) [32], Nashville (0.025) [17]. A much higher value (0.091) was reported by a recent study in western China [12], possibly because the important precursors of PAN, ethane, propene, and olefins, were dominant VOC species in LZ airshed.

As general products of photochemistry, the formation mechanism of O_3 and PAN are closely linked [26], and good correlations have been found during numerous studies [7,14,13,28,33]. The results of this work are shown in Figure 5. A moderate correlation between O_3 and PAN was found, with linear regression coefficient $R = 0.73$. According to [16], the intercept of the linear regression line of O_3/PAN can reveal the background mixing ratio of O_3. PAN is prone to thermo dissociation and sensitive to the ambient temperature. From this concern, ambient temperature may lower the ratio of PAN and O_3. Actually, the dependence of PAN levels with temperature is more complex. At day-time, the formation and loss processes both exit. The variation of PAN is the net result of both effects. Although higher temperature tends to destruct PAN molecules faster, positive correlation between daily maximums of temperature and PAN has been found by many studies [e.g. 24]. In the same work, similar positive correlation was also found between daily maximums of temperature and O_3. Therefore, temperature may have little effect on lower PAN/O_3, and ambient data could be directly used for discussion [12].

In this study, from the intercept in Figure 5, the background level of O_3 was estimated to be 28 ppbv (±15 ppbv). This value is comparable to the result by [3], in which about 30 ppbv was measured to be the background O_3 level of the continent outflow. According to the review by Vingarzan [34], annual average background O_3 levels over the mid-latitudes of the Northern Hemisphere range between 20 and 45 ppbv, and increase with

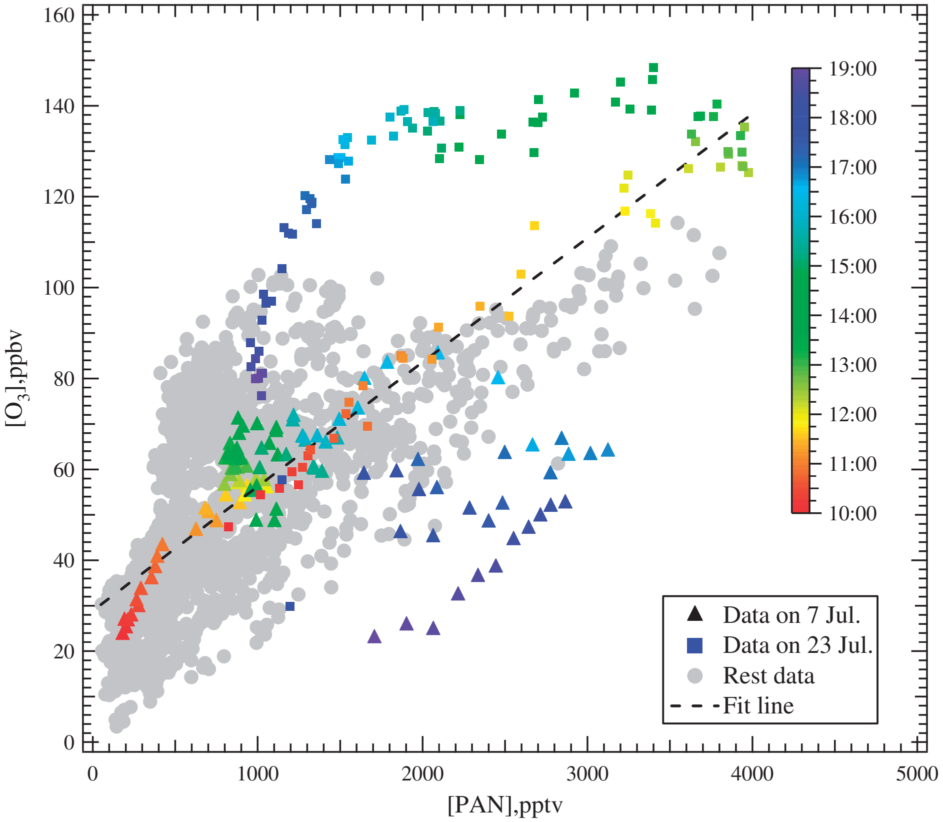

Figure 5. Correlation between PAN and Ozone. The solid grey circles show the data from 10:00 to 19:00 of the whole campaign except 7 July and 23 July which are demonstrated by solid triangles and solid squares, respectively. The data on these two days are also interpreted by time colour-scales. The dashed line is the fit line of Ozone and PAN, with the equation of $[O_3] = 0.27\ [PAN] + 28.88$.

a speed of 0.5–2% per year. In addition, this value was also in good agreement with that reported by a 14-year measurement at a background site Hok Tsui in PRD [35]. Thus, 28 ppbv (±15 ppbv) is reasonable for the regional background O_3 level in PRD.

3.4 *Case study*

3.4.1 *Night-time transportation of secondary pollutants from Guangzhou city*

Night-time peaks of PANs were believed to be the evidence for air mass transport [12]. In this study, high night-time PAN plumes were measured on 21 July and 23 July (Figure 2c and d). Both plumes were observed around midnight, at 21:00–23:00 (LT) on 21 July and 0:00–3:00 (LT) on 23 July. The mixing ratio of PAN and PPN were even higher than the day-time maxima on 21 July. Although O_3 increased with PANs, since there was no light during such time, the increase of the secondary pollutants could not be caused by local photochemical production. The decrease of the planetary boundary layer (PBL) during nights could increase mixing ratios of air pollutants. If this was the reason,

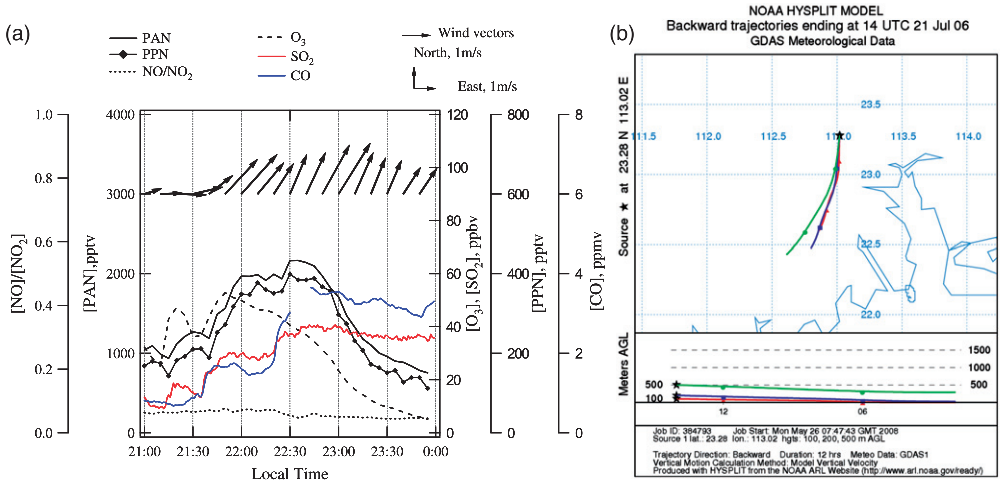

Figure 6. (a) Night-time peaks on 21 July. Black arrows show the wind vectors; the dotted line shows the variation of NO/NO_2; the dashed line is O_3; the blue line is CO; the red line is SO_2; the solid line is mixing ratios of PAN; and the solid line with black diamonds is PPN. (b) 12 hours back trajectories computed by Hysplit Model (NOAA), showing the plumes which reach BGS at 22:00 21 July (LT).

all the air pollutants should show similar variation. However, as shown in Figure 6a, while CO and SO_2 varied in the same way, PAN, PPN, and O_3 showed very different patterns. Thus, the change of PBL was not the reason of the detection of high level secondary pollutants.

The pollutants could be transported from upwind areas, and the backward trajectory computed by HYSPLIT was used as a tool to explore the transport pathways and possible source regions. As shown in Figure 6a, the ratio of NO/NO_2 was lower than 0.1, indicating the air mass had been highly photochemical processed. The timing of elevated PANs and O_3 corresponded very well with the local wind vectors. The back trajectories computed by HYSPLIT (NOAA) revealed that the air parcel was moving at ground level, and passed the Guangzhou metropolitan area 8 hours before they arrived at the sampling site (Figure 6b). Therefore, it is reasonable to conclude that the pollutants contained in the plume were formed at Guangzhou during the day-time, and transported to the BGS and detected at nights.

The very similar event of the transportation was also found during 0:00–3:00 (Beijing time) on 23 July, hinting that impact of urban plumes to the receptor site could be an important issue in understanding variations of PANs.

3.4.2 *Day-time impacts from anthropogenic VOCs*

Two day-time episodes of 7 July and 23 July were well identified in the campaign, as indicated by the ratio PPN/PAN in Figure 3. Both episodes were showing significant influence from anthropogenic sources. July 7 showed a shift from BVOCs to AVOCs dominance, and strong impacts of fresh emissions. However, 23 July showed a severe photochemical O_3 pollution dominated by AVOCs.

(1) Episode 7 July day-time shifting from BVOCs to AVOCs dominance. As illustrated by the colour-scale in Figure 3, the locally emitted BVOCs were dominating the

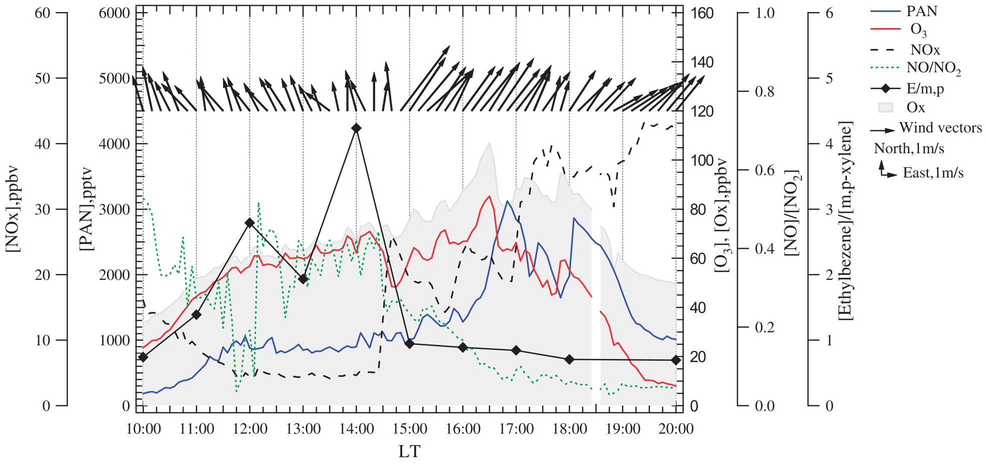

Figure 7. Day-time episode of 7 July, showing PAN the blue line, Ozone the red line, wind vectors the black arrows, NOx the dashed line, NO/NO_2 the green dotted line, Ox the shaded area, and Ethylbenzene/m,p-xylene the black solid line and solid diamonds.

photochemistry of PAN production at noon. The ratios of PPN/PAN between 12:00 and 14:30 were lower than 10%, indicating BVOCs dominance. This was a common phenomenon since BVOC emissions were highly correlated with temperature and solar radiation which were strongest during noon. These points corresponded to medium levels of O_3, lower than the second level criterion of NAAQS.

After 14:45, the PAN photochemistry shifted to AVOCs dominance, and lasted to the end of the episode. The ratios of PPN/PAN increased to much higher than 10%. This phenomenon was following the rapid change of wind direction, which turned from ‘south-southeast’ to ‘southwest’ with much higher speed (arrows in Figure 7). A sharp increase in NOx (from 5 ppbv to 25 ppbv) and decrease in O_3 (from 65 ppbv to 48 ppbv) was observed in the next 15 minutes. In the following hour, NOx and O_3 showed almost opposite trends, while the total oxidants (Ox, $Ox = NO_2 + O_3$ in this study) was growing steadily. This process is often attributed to the impact of the fresh emission of NOx [36]. The photochemical age indicated by ethylbenzene/m,p-xylene showed a similar sudden decrease almost at the same time and stayed at a low level in later hours, suggesting that the plume mainly consisted of fresh primary pollutants. All these changes were associated with the rapid change in wind direction and therefore in sources and atmospheric pathways between emissions and the sampling site, indicating that the plume was transported from an area with abundant anthropogenic emissions, which probably was the industrial area in the west of Guangzhou city.

(2) Episode 23 July severe O_3 pollution. On this day, the most severe pollution in this campaign was recorded. The highest mixing ratio of O_3 and PAN were measured, and ground level O_3 stayed above 80 ppbv for nearly 8 hours and above 100 ppbv for more than 6 hours. PPN/PAN ratio was almost 17% at noon (indicating by the colour-scale in Figure 3), implying that AVOCs were dominant in the photochemical processes even when local BVOCs emissions were strongest in the day. Based on the discussion on 7 July, the possibility of local PAN formation could be excluded. If PAN was formed locally, it must

show a strong influence from BVOCs at noon, and PPN/PAN should be similar to that on 7 July. Given the fact that the air mass was very stagnant (wind speed $<1\,\mathrm{m\,s^{-1}}$), and Guangzhou city was the nearest most possible source, this phenomenon was probably attributed to the dispersion of pollutants from Guangzhou city to suburban and rural areas.

4. Conclusions

PAN and PPN were continuously measured at a BGS as part of the PRIDE-PRD2006 campaign. This was the first time that they were measured in this region. Both of them showed obvious diurnal patterns. The mixing ratios were comparable with that of Beijing city, but much lower than Mexico City and Santiago.

PANs were good indicators for understanding O_3 pollution. By the correlation coefficient and the slope of the linear regression line of PPN/PAN, AVOCs were dominating the O_3 production process. By the intercept of the linear regression line of O_3/PAN, the background O_3 level was estimated to be 28 ppbv (±15 ppbv). However, since MPAN (peroxymethacryloyl nitrate), the distinct indicator for BVOCs, was not measured, the role of BVOCs could not be discussed in this study.

The BGS was heavily impacted by pollutants transported from Guangzhou city. Two night-time plumes containing elevated PAN were observed, which were highly photochemically processed and carrying a large magnitude of secondary pollutants. Two typical day-time episodes were well identified, both showing strong influence from Guangzhou city. To know more about the regional O_3 problem and impacts from megacities to suburban and rural areas, PAN, PPN and MPAN should be simultaneously measured and analysed at more sites in the PRD.

Acknowledgements

This work was supported by The National High Technology Research and Development Program of China (863 Program) 2006AA06A301, and the China National Basic Research and Development Program 2002CB410801. The authors thank Cheng-Hsun Lai for VOCs data.

References

[1] T. Wang, C.N. Poon, Y.H. Kwok, and S.Y. Li, Atmos. Environ. (AE International – Asia) **37**, 3539 (2003).
[2] K.L. So and T. Wang, Environ. Pollut. **123**, 307 (2003).
[3] T. Wang, H. Gou, D.R. Blake, Y.H. Kwok, I.J. Simpson, and Y.S. Li, J. Atmos. Chem. **52**, 295 (2005).
[4] W.W. Heck, O.C. Taylor, R. Adams, G. Bingham, J. Miller, E. Preston, and L. Weinstein, J. Air Waste Mange. Assoc. **32**, 353 (1982).
[5] J.N. Woodman and E.B. Cowling, Environ. Sci. Technol. **21**, 120 (1987).
[6] L.J. Folinsbee, W.F. McDonnell, and D.H. Horstman, J. Air Waste Mange. Assoc. **38**, 28 (1988).
[7] E. Grosjean, D. Grosjean, and L.F. Woodhouse, Environ. Sci. Technol. **35**, 4007 (2001).
[8] H. Tanimoto and H. Akimoto, Geophys. Res. Lett. **28**, 2831 (2001).
[9] J.M. Roberts, F. Flocke, A. Weinheimer, H. Tanimoto, B.T. Jobson, D. Riemer, E. Apel, E. Atlas, S. Donnelly, V. Sroud, K. Johnson, R. Weaver, and F.C. Fehsenfeld, Geophys. Res. Lett. **28**, 4195 (2001).

[10] J.B. Zhang and X.Y. Tang, Environ. Chem. (in Chinese) **1**, 30 (1990).

[11] J. Williams, J.M. Roberts, S.B. Bertman, C.A. Stroud, F.C. Fehsenfeld, K. Baumann, M.P. Buhr, K. Knapp, P.C. Murphy, M. Nowick, and E.J. Williams, J. Geophys. Res. **105**, 28943 (2000).

[12] J.M. Zhang, T. Wang, A.J. Ding, X.H. Zhou, L.K. Xue, C.N. Poon, W.S. Wu, J. Gao, H.C. Zuo, J.M. Chen, X.C. Zhang, and S.J. Fan, Atmos. Environ. **43**, 228 (2009).

[13] B. Wang and J.B. Zhang, Environ. Sci. (in Chinese) **28**, 1621 (2007).

[14] J.S. Gaffney, N.A. Marley, M.M. Cunningham, and P.V. Doskey, Atmos. Environ. **33**, 5003 (1999).

[15] J.M. Roberts, C.A. Stroud, B.T. Jobson, M. Trainer, D. Hereid, E. Williams, F. Fehsenfeld, W. Brune, M. Martinez, and H. Harder, Geophys. Res. Lett. **28**, 4583 (2001).

[16] J. Williams, J.M. Roberts, F.C. Fehsenfeld, S.B. Bertman, M.P. Buhr, P.D. Goldan, G. Huebler, W.C. Kuster, T.B. Ryerson, M. Trainer, and V. Young, Geophys. Res. Lett. **24**, 1099 (1997).

[17] J.M. Roberts, F. Flocke, C.A. Stroud, D. Hereid, E. Williams, F. Fehsenfeld, W. Brune, M. Martinez, and H. Harder, J. Geophys. Res. **107**, 4554 (2002).

[18] H.B. Singh and P.L. Hanst, Geophys. Res. Lett. **8**, 941 (1981).

[19] D. Grosjean, Environ. Sci. Technol. **17**, 13 (1983).

[20] H.B. Singh, L.J. Salas, B.A. Ridley, J.D. Shetter, N.M. Donohue, F.C. Fehsenfeld, D.W. Fahey, D.D. Parrish, E.J. Williams, S.C. Liu, G. Huebler, and P.C. Murphy, Nature **318**, 347 (1985).

[21] H.W. Jacobi and O. Schrems, Phys. Chem. Chem. Phys. **1**, 5517 (1999).

[22] H.B. Singh and L.J. Salas, Atmos. Environ. **23**, 231 (1989).

[23] H.J. Beine and T. Krognes, Atmos. Environ. **34**, 933 (2000).

[24] J.M. Roberts, F. Flocke, G. Chen, J. de Gouw, J.S. Holloway, G. Hueber, A. Neuman, D.K. Nicks Jr, J.B. Nowak, D.D. Parrish, T.B. Ryerson, D.T. Sueper, C. Wameke, and F.C. Fensenfeld, J. Geophys. Res. **109**, D23S21 (2004).

[25] B. Rappenglueck, C. Forster, G. Jakobi, and M. Pesch, Atmos. Environ. **38**, 6125 (2004).

[26] J.M. Roberts, J. Williams, K. Baumann, M.P. Buhr, P.D. Goldan, J. Holloway, G. Huebler, W.C. Kuster, S.A. Mckeen, T.B. Ryerson, M. Trainer, E.J. Williams, F.C. Fehsenfeld, S.B. Bertman, G. Nouaime, C. Seaver, G. Grodzinsky, M. Rodgers, and V.L. Young, J. Geophys. Res. **103**, 22437 (1998).

[27] L.K. Whalley, A.C. Lewis, J.B. McQuaid, P.M. Purvis, J.D. Lee, K. Stemmler, C. Zellweger, and P. Ridgeon, J. Environ. Monit. **6**, 234 (2004).

[28] M.A. Rubio, P. Oyola, E. Gramsch, E. Lissi, J. Pizarro, and G. Villena, Atmos. Environ. **38**, 4931 (2004).

[29] D. Grosjean, E.L. Williams II, and E. Grosjean, Environ. Sci. Technol. **27**, 979 (1993).

[30] J.A. de Gouw, A.M. Middlebrook, C. Warneke, P.D. Goldan, W.C. Kuster, J.M. Roberts, F.C. Fehsenfeld, D.R. Worsnop, M.R. Canagaratna, A.A.P. Pszenny, W.C. Keene, M. Marchewka, S.B. Bertman, and T.S. Bates, J. Geophys. Res. **110**, D16305 (2005).

[31] V. Librando and G. Tringali, J. Environ. Man. **75**, 275 (2005).

[32] N.A. Marley, J.S. Gaffney, R. Ramos-Villegas, and B. Cárdenas González, Atmos. Chem. Phys. **7**, 2277 (2007).

[33] A.P. Altshuller, Atmos. Environ. **17**, 2383 (1983).

[34] R. Vingarzan, Atmos. Environ. **38**, 3431 (2004).

[35] T. Wang, X.L. Wei, A.J. Ding, C.N. Poon, K.S. Lam, Y.S. Li, L.Y. Chan, and M. Anson, Atmos. Chem. Phys. Discuss. **9**, 10429 (2009).

[36] J.M. Roberts, M. Marchewka, S.B. Bertman, R. Sommariva, C. Warneke, J. de Gouw, W. Kuster, P. Goldan, E. Williams, B.M. Lerner, P. Murphy, and F.C. Fensenfeld, J. Geophys. Res. **112**, D20306 (2007).